Asian Journal of Chemistry; Vol. 23, No. 5 (2011), 2261-2265

ASIAN JOURNAL OF CHEMISTRY

www.asianjournalofchemistry.co.in

Microwave-Assisted Metathetic Synthesis of Ag-MWO_4/Zeolite-A (M = Co, Ni) Porous Composites†

C.S. LIM

Department of Advanced Materials Science and Engineering, Hanseo University, Seosan 356-706, South Korea

Corresponding author: Tel/Fax: +82 41 6601445; E-mail: cslim@hanseo.ac.kr

AJC-9544

Ag-MWO_4/zeolite-A (M = Co, Ni) porous composites were synthesized using a solid-state metathetic (SSM) method with microwave irradiation. The characteristics of the solid-state metathetic reaction and the formation of the high lattice energy by-product NaCl were found to drive the reaction for wolframite-type $CoWO_4$ and $NiWO_4$ toward completion. The Ag-MWO_4/zeolite-A (M = Co, Ni) porous composites were formed completely at 600 °C. Monoclinic-like crystals of $CoWO_4$ and $NiWO_4$ were primarily co-mixed with porous zeolite-A. Small spherical silver particles were immobilized in the porous MWO_4/zeolite-A (M = Co, Ni) matrix.

Key Words: Solid-state metathetic, Synthesis, Ag-MWO_4/Zeolite-A (M = Co, Ni), Porous composites, Microwave irradiation.

INTRODUCTION

Metal tungstates with large bivalent cations (*e.g.*, Ca, Ba, Pb and Sr) tend to have a scheelite-type tetragonal structure, whereas small cationic radii (*e.g.*, Zn, Fe, Mn, Co and Ni) favour the formation of a wolframite-type monoclinic structure. The main difference between the two structures is that every tungeston atom is surrounded by four O atoms in a scheelite-type structure, whereas six O atoms surround every tungeston atom in metal tungstate crystallizing in the wolframite-type structure[1,2].

In recent years, metal tungstates have attracted considerable attention for potential applications as a scintillator, microwave devices, luminescent material and photocatalyst[3-7]. The physical, chemical and photochemical properties of metal tungstates are dependent on the manufacturing method. Several processes have been developed over the past decade to enhance the applications of $CoWO_4$ and $NiWO_4$. $CoWO_4$ and $NiWO_4$ are prepared by a range of processes, such as solid-state reactions[8,9], co-precipitations[10-12], from molten salts[13,14], from hydrothermal reactions[15,16], by combustion[17], a mechano-chemical method[18], from a polymeric precursor[19], by microwave irradiations[20-22]. Compared with the usual methods, the microwave synthesis has the advantages of a very short reaction time, small particle size, narrow particle size distribution and high purity method for preparing polycrystalline samples. Among these methods, the solution-based chemical synthetic methods play a key role in the design and production of fine ceramics and have been successful in overcoming many of the limitations of traditional solid-state, high-temperature methods. In addition, the use of solution chemistry can eliminate major problems, such as long diffusion paths, impurities and agglomeration, which result in products with improved homogeneity.

Wet chemical methods have disadvantages, such as complicated synthetic steps, use of expensive equipment, high synthetic temperature and long sintering times. On the other hand, the solid-state reaction requires complex apparatus and techniques, which are becoming gradually unpopular due to excessive energy consumption. However, solid-state synthesis of materials by the metathetic route is a simple method of synthesis, cost-effective, high yield and easy scale up and is emerging as a viable alternative approach for synthesizing high-quality novel inorganic materials in a short time[23,24]. The solid state metathetic approach assisted by microwave irradiation has been applied successfully to the synthesis of metal tungstate of wolframite-type MWO_4 (M = Zn, Mn, Ni) and scheelite-type MWO_4 (M = Ca, Sr, Ba)[25], $ZrCr_2O_4$[26], $ZnSiO_4$ and $MCrO_4$ (M = Ca, Sr, Ba, Pb)[27] and $MMoO_4$ (M = Ca, Sr, Ba)[28, 29]. Ag-incorporated MWO_4/zeolite-A porous composites are expected to have excellent adsorption and synergy effects in an immobilization mechanism of metallic catalysts for a wide range of applications, such as sensors, photocatalysts, luminescence, anti-bacterial matrices and optical effects in the UV and visible region.

In this study, Ag-MWO_4/zeolite-A (M = Co, Ni) porous composites were synthesized using a solid-state metathetic

---

†Presented to the 4th Korea-China International Conference on Multi-Functional Materials and Application.

(SSM) method with microwave irradiation. The characteristics of the SSM reaction and the formation of a high lattice energy by-product NaCl were discussed. The Ag-MWO_4/zeolite-A (M = Co, Ni) porous composites were immobilized from mixed metathetic precursors at moderate temperatures. The crystallization process, thermal decomposition and morphology of the synthesized Ag-MWO_4/zeolite-A (M = Co, Ni) porous composite powders were evaluated.

EXPERIMENTAL

Fig. 1 shows a flow chart for the synthesis of Ag-MWO_4/zeolite-A (M = Co, Ni) porous composites from the solid-state metathetic method using microwave irradiation. $CoCl_2·6H_2O$, $NiCl_2·6H_2O$ and $Na_2WO_4·2H_2O$ were used to prepare the metal tungstate compound. The preparation of metal tungstates were carried out by reacting well-ground mixtures of $CoCl_2·6H_2O$ and $Na_2WO_4·2H_2O$ for $CoWO_4$ and $NiCl_2·6H_2O$ and $Na_2WO_4·2H_2O$ for $NiWO_4$ at a molar ratio of 1:1. The sample mixtures were dried at 100 °C for 12 h and 5 wt % $AgNO_3$ and 25 wt % synthetic zeolite-A were then added. The samples were placed into crucibles and exposed to domestic microwave (Samsung Electronics Corp. Korea) operating at a frequency of 2.45 GHz and a maximum out-put power of 1250 W for 10 min. The samples were treated with ultrasonic radiation and washed many times with distilled water and ethanol to remove the sodium chloride reaction by-product. The samples were dried at 100 °C in an oven. Heat-treatment of the samples was performed at 600 °C for 3 h.

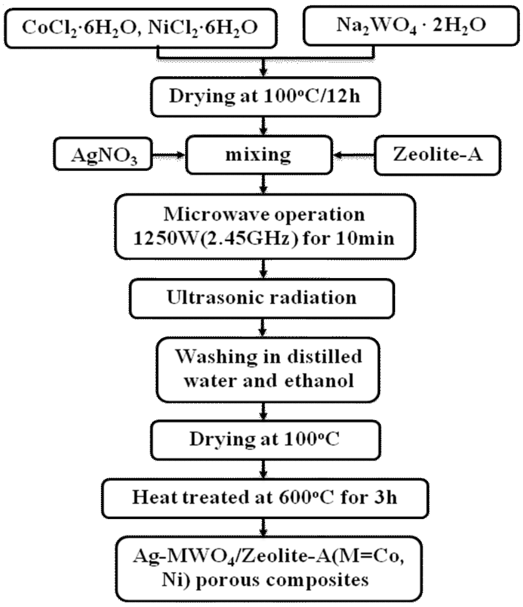

Fig. 1. Flow chart for the synthesis of Ag-MWO_4/zeolite-A (M = Co, Ni) porous composites from the SSM method using microwave irradiation

The crystallization of the existing phase in the powders after heat-treatment was examined by powder X-ray diffraction (XRD, CuK_{α}, 40 kV, 30 mA, Rigaku, Japan) at a scan rate of 3 °/min. Fourier transform infrared spectroscopy (FT-IR, Model IR 550, Magna, Nicolet Company) was used to examine the thermal-decomposition behaviour of the metathetic reaction and heat-treated powders over frequency range, 4000-400 cm^{-1}. The FT-IR spectra were measured in KBr pellets. The microstructure and surface morphology of the Ag-MWO_4/zeolite-A (M = Co, Ni) porous composite powders were observed by scanning electron microscopy (SEM, JSM-35CF, JEOL) and energy-dispersive X-ray spectroscopy (EDS).

RESULTS AND DISCUSSION

Fig. 2 shows XRD patterns of the Ag-$CoWO_4$/zeolite-A porous composites heat-treated at 600 °C for 3 h. The XRD patterns are indexed on basis of the crystallographic data of the structure of $CoWO_4$ (JCPDS code 15-0867) and other contained peaks corresponding to the co-mixed structure of Ag(Ag*) and zeolite-A(Z). The major peak intensities were higher and confirmed that the phases were wolframite $CoWO_4$. Fig. 3 shows XRD patterns of the Ag-$NiWO_4$/zeolite-A porous composites heat-treated at 600 °C for 3 h. The XRD patterns are indexed on basis of the crystallographic data of the structure of $NiWO_4$ (JCPDS code 15-0755) and other contained peaks corresponding to the co-mixed structure of Ag(Ag*) and zeolite-A(Z). The major peak intensities were higher and confirmed that the phases were wolframite $NiWO_4$. The formations of $FeWO_4$ and $NiWO_4$ crystalline phases were needed to heat at 600 °C for 3 h. The tungstates follow a wolframite monoclinic crystal structure. Their lattice parameters as follows: a = 4.670 Å, b = 5.687 Å, c = 4.951 Å and β = 90.0° for $CoWO_4$ [Ref. 2] and a = 4.599 Å, b = 5.66 Å, c = 4.906 Å and β = 90.03° for $NiWO_4$ [Ref. 25]. It indicates that the solid-state metathetic synthesis is adequate for the growth of $FeWO_4$ and $NiWO_4$ crystallites and development of Ag-$CoWO_4$/zeolite-A and Ag-$NiWO_4$/zeolite-A porous composites.

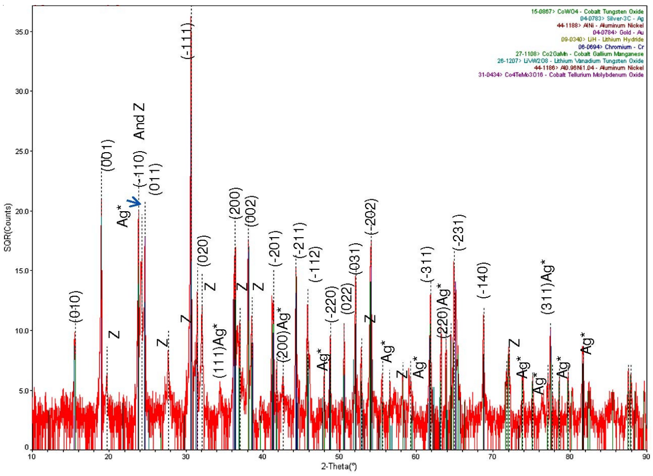

Fig. 2. XRD patterns of the Ag-$CoWO_4$/zeolite-A porous composites heat-treated at 600 °C for 3 h

Fig. 4 shows FT-IR spectra of the Ag-$CoWO_4$/zeolite-A porous composites after (a) microwave metathetic reaction (Ag-$CoWO_4$-Z-m) and (b) heat-treated at 600 °C for 3 h (Ag-$CoWO_4$-Z-m600). The absorption bands at 473 and 532 cm^{-1} can be assigned to symmetric and asymmetric deformation mode of Co-O in CoO_6 octahedra. The absorption bands with their maxima at 633 and 710 cm^{-1} can be due to the stretching modes of W-O in WO_6 octahedra. The bands at 834 and 877 cm^{-1} were due to symmetrical vibrations of bridge oxygen

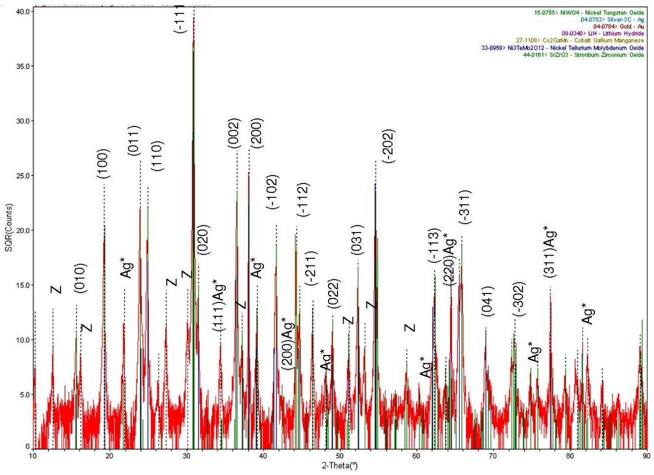

Fig. 3. XRD patterns of the Ag-NiWO$_4$/zeolite-A porous composites heat-treated at 600 ºC for 3 h

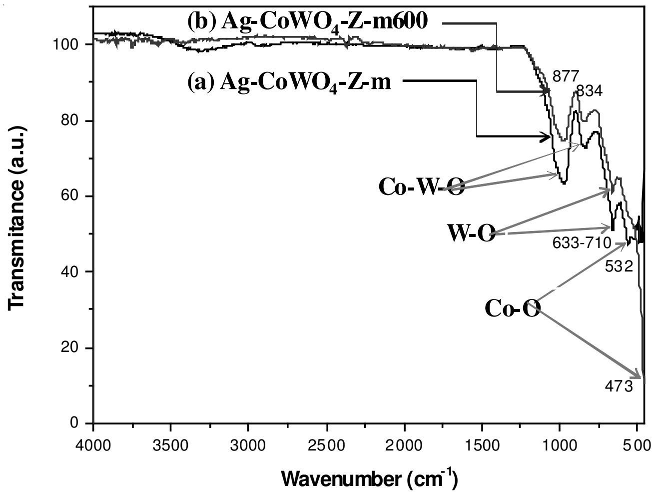

Fig. 4. FT-IR spectra of the Ag-CoWO$_4$/zeolite-A porous composites after (a) microwave metathetic reaction and (b) heat-treated at 600 ºC for 3 h

atoms of the Co-O-W groups. These vibrations could be identified to the synthesized FeWO$_4$. The small band at 1450 and 1630 cm^{-1} can in Fig. 4(a) Ag-CoWO$_4$-Z-m are assigned to the HOH bending vibrations. It is assumed that the samples prepared contain a significant amount of surface-adsorbed water and alcohol.

Fig. 5 shows FT-IR spectra of the Ag-NiWO$_4$/zeolite-A porous composites after (a) microwave metathetic reaction (Ag-NiWO$_4$-Z-m) and (b) heat-treated at 600 ºC for 3 h (Ag-NiWO$_4$-Z-m 600). The absorption bands at 532 cm^{-1} can be assigned to symmetric and asymmetric deformation mode of Ni-O in NiO$_6$ octahedra. The absorption bands with their maxima at 633 and 710 cm^{-1} can be due to the stretching modes of W-O in WO$_6$ octahedra. The bands at 834 and 877 cm^{-1} were due to symmetrical vibrations of bridge oxygen atoms of the Ni-O-W groups. These vibrations could be identified to the synthesized NiWO$_4$. The band at 1630 cm^{-1} can in Fig. 5(a) Ag-NiWO$_4$-Z-m are assigned to the HOH bending vibrations. It is assumed that the samples prepared contain a significant amount of surface-adsorbed water and alcohol. Obviously, the bands at 1630 cm^{-1} disappeared after heat-treated at 600 ºC for 3 h in Fig.5(b) Ag-NiWO$_4$-Z-m 600.

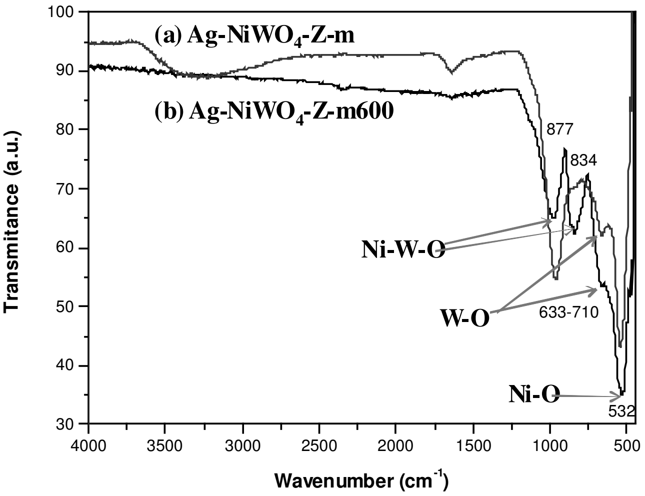

Fig. 5. FT-IR spectra of the Ag-NiWO$_4$/zeolite-A porous composites after (a) microwave metathetic reaction and (b) heat-treated at 600 ºC for 3 h

Fig. 6 shows SEM images of the Ag-CoWO$_4$/zeolite-A porous composites after (a) microwave metathetic reaction and (b) heat-treated at 600 ºC for 3 h and Ag-NiWO$_4$/zeolite-A porous composites after (c) microwave metathetic reaction and (d) heat-treated at 600 ºC for 3 h. Fig. 6(a) and (c) shows SEM images of the Ag-CoWO$_4$/zeolite-A and Ag-NiWO$_4$/zeolite-A porous composites synthesized by SSM reaction after removing the NaCl. CoWO$_4$ and NiWO$_4$ crystallize in wolframite crystal structures. Presence of sodium chloride confirms the reaction has proceeded in solid-state metathesis way. Parhi *et al.*[25] reported the microwave metathetic synthesis of various metal tungstates and showed that microwave radiation provided the energy required to overcome the energy barrier that precludes a spontaneous reaction and helped heat the bulk of the material uniformly, resulting in fine particles with a controlled morphology and the formation of the product in a green manner without the generation of solvent waste.

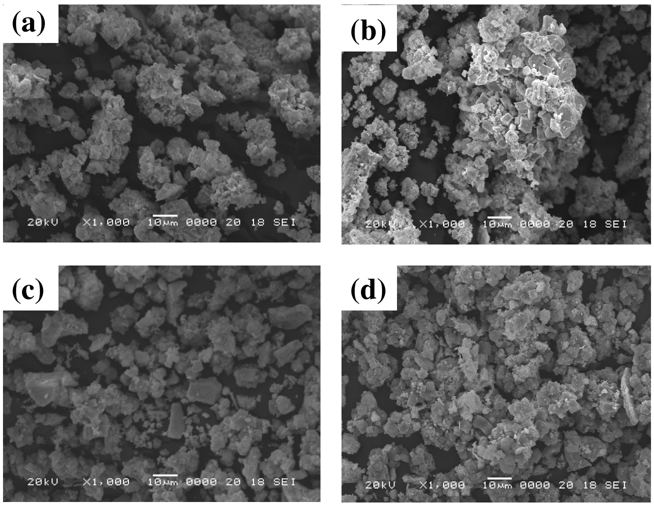

Fig. 6. SEM images of the Ag-CoWO$_4$/zeolite-A porous composites after (a) microwave metathetic reaction and (b) heat-treated at 600 ºC for 3 h and Ag-NiWO$_4$/zeolite-A porous composites after (c) microwave metathetic reaction and (d) heat-treated at 600 ºC for 3 h

In Fig. 6(b) and (d), the SEM images of Ag-CoWO$_4$/zeolite-A and Ag-NiWO$_4$/zeolite-A porous composites heat-treated at 600 ºC for 3 h show the well crystallized $CoWO_4$ and $NiWO_4$ on the zeolite-A synthesized by a SSM reaction. The monoclinic-like crystals of $CoWO_4$ and $NiWO_4$ were primarily co-mixed with Ag on the porous zeolite-A surfaces. The spherical small particles of silver were well immobilized in the porous $CoWO_4$/zeolite-A and $NiWO_4$/zeolite-A composites matrix. Solid state metathesis reactions, such as $ACl_2 + Na_2WO_4 \rightarrow AWO_4 + 2NaCl$, involves the exchange of atomic/ionic species, where the driving force is the formation of thermodynamically stable alkali or alkaline earth halides with high lattice energy. The thermodynamic basis for such metathetic reactions has been reported[25,30-32]. Parhi *et al.*[24] calculated the enthalpy (ΔH) and free energy change (ΔG) associated with the formation of tungstates and reported ΔH = -36.17 KJ/mol for $ZnWO_4$ showing that both the enthalpy change favours the metathesis reaction and the enthalpy change is indeed the driving force for the metathesis involving the formation of NaCl. SSM reactions occur so rapidly that all the enthalpy released is essentially used to heat up the solid products, usually raising the alkali halide near or above its normal boiling point and have been recognized to be approximately adiabatic in nature[33].

Fig. 7 shows (a) EDS patterns, (b) quantitative compositions, (c) a SEM image and (d) quantitative results of the synthesized Ag-$CoWO_4$/zeolite-A porous composites at 600 ºC for 3 h. The EDS patterns and quantitative compositions of the synthesized Ag-$CoWO_4$/zeolite-A porous composites were composed of Ag, $CoWO_4$ and zeolite-A. Fig. 8 shows (a) EDS patterns, (b) quantitative compositions, (c) a SEM image and (d) quantitative results of the synthesized Ag-NiWO4/zeolite-A porous composites at 600 ºC for 3 h. The EDS patterns and quantitative compositions of the synthesized Ag-$NiWO_4$/zeolite-A porous composites were composed of Ag, $NiWO_4$ and zeolite-A.

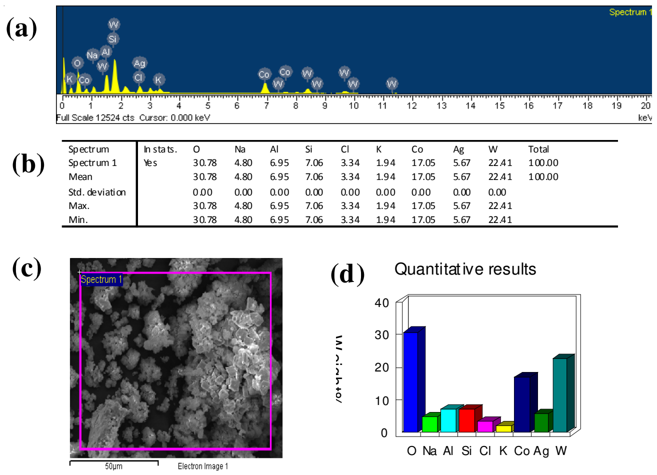

Spectrum	In stats.	O	Na	Al	Si	Cl	K	Co	Ag	W	Total
Spectrum 1	Yes	30.78	4.80	6.95	7.06	3.34	1.94	17.05	5.67	22.41	100.00
Mean		30.78	4.80	6.95	7.06	3.34	1.94	17.05	5.67	22.41	100.00
Std. deviation		0.00	0.00	0.00	0.00	0.00	0.00	0.00	0.00	0.00	
Max.		30.78	4.80	6.95	7.06	3.34	1.94	17.05	5.67	22.41	
Min.		30.78	4.80	6.95	7.06	3.34	1.94	17.05	5.67	22.41	

Fig. 7. EDS patterns (a), quantitative compositions (b), a SEM image (c) and quantitative results (d) of the synthesized Ag-$CoWO_4$/zeolite-A porous composites

For tungstate materials to be used for practical applications, versatile characteristics are required for the particle size distribution and morphology of the particles. The well-defined particle features of the Ag-$CoWO_4$/zeolite-A and Ag-$NiWO_4$/zeolite-A porous composites synthesized by SSM reactions have control over the morphology of the final particles and can be used for such technological applications. Owing to the enthalpy change by the driving force for the metathetic formation of NaCl, the SSM reactions affect not only the morphology of the $CoWO_4$ and $NiWO_4$ particles, but also the formation of functional zeolite and Ag immobilized in the porous composite matrix. Therefore, a variation of metathetic reactions of $MCl_2 + Na_2WO_4 \rightarrow MWO_4 + 2NaCl$ is required to control the well-defined particle features of the Ag-MWO_4/zeolite-A (M = Co, Ni) porous composites.

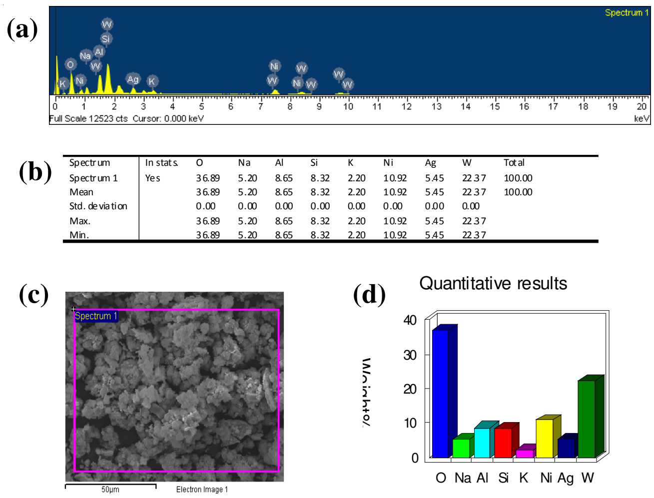

Spectrum	In stats.	O	Na	Al	Si	K	Ni	Ag	W	Total
Spectrum 1	Yes	36.89	5.20	8.65	8.32	2.20	10.92	5.45	22.37	100.00
Mean		36.89	5.20	8.65	8.32	2.20	10.92	5.45	22.37	100.00
Std. deviation		0.00	0.00	0.00	0.00	0.00	0.00	0.00	0.00	
Max.		36.89	5.20	8.65	8.32	2.20	10.92	5.45	22.37	
Min.		36.89	5.20	8.65	8.32	2.20	10.92	5.45	22.37	

Fig. 8. EDS patterns (a), quantitative compositions (b), a SEM image (c) and quantitative results (d) of the synthesized Ag-$NiWO_4$/zeolite-A porous composites

Conclusion

Ag-MWO_4/zeolite-A (M = Co, Ni) porous composites were synthesized using solid-state metathetic (SSM) method with microwave irradiation. The Ag-MWO_4/zeolite-A (M = Co, Ni) porous composites at 600 ºC for 3 h were completed entirely at 600 ºC. The well crystallized $CoWO_4$ and $NiWO_4$ on the zeolite-A synthesized by a SSM reaction. The monoclinic-like crystals of $CoWO_4$ and $NiWO_4$ were primarily co-mixed with Ag on the porous zeolite-A surfaces. The spherical small particles of silver were well immobilized in the porous $CoWO_4$/zeolite-A and $NiWO_4$/zeolite-A composites matrix. The enthalpy change favours the metathesis reaction and the enthalpy change is indeed the driving force for the metathesis involving the formation of NaCl. Solid-state metathetic reactions occur so rapidly that all the enthalpy released is essentially used to heat up the solid products of Ag-MWO_4/zeolite-A (M = Co, Ni) porous composites.

ACKNOWLEDGEMENTS

This study was supported by Basic Science Research Program through the National Research Foundation of Korea (NRF) funded by the Ministry of Education, Science and Technology (2010-0023911).

REFERENCES

1. S. Rajagopal, D. Nataraj, O.Y. Khyzhun, Y. Djaoued, J. Robichaud and D. Mangalaraj, *J. Alloys Comp.*, **493**, 340 (2010).
2. S. Rajagopal, V.L. Bekenev, D. Nataraj, D. Mangalaraj and O.Y. Khyzhun, *J. Alloys Comp.*, **496**, 61 (2010).

3. X. Cao, W. Wu, N. Chen, Y. Peng and Y. Liu, *Sen. Actuators B*, **137**, 83 (2009).
4. C. Yu and J.C. Yu, *Mater. Sci. Eng. B*, **164**, 16 (2009).
5. S. Lin, J. Chen, X. Weng, L. Yang and X. Chen, *Mater. Res. Bull.*, **44**, 1102 (2009).
6. P.K. Pandy, N.S. Bhave and R.B. Kharat, *J. Mater. Sci.*, **42**, 7927 (2007).
7. R.P. Jia, G.X. Zhang, Q.S. Wu and Y.P. Ding, *Mater. Lett.*, **61**, 1793 (2007).
8. S.M. Montemayeor and A.F. Fuentes, *Ceram. Int.*, **30**, 393 (2004).
9. S.J. Naik and A.V. Salker, *Solid State Sci*., **12**, 2065 (2010).
10. T. Montini, V. Gombac, A. Hameed, L. Felisari, G. Adami and P. Fornasiero, *Chem. Phys. Lett.*, **498**, 113 (2010).
11. T. You, G. Cao, X. Song, C. Fan, W. Zhao, Z. Yin and S. Sun, *Mater. Lett.*, **62**, 1169 (2008).
12. A. Sen and P. Pramanik, *J. Eur. Ceram. Soc.*, **21**, 745 (2001).
13. Z. Song, J. Ma, H. Sun, W. Wang, Y. Sun, L. Sun, Z. Liu and C. Gao, *Ceram. Int.*, **35**, 2675 (2009).
14. Z. Song, J. Ma, H. Sun, Y. Sun, J. Fang, Z. Liu, C. Gao, Y. Liu and J. Zhao, *Mater. Sci. Eng. B*, **163**, 62 (2009).
15. D. Chen, G. Shen, K. Tang, H. Zheng and Y. Qian, *Mater. Res. Bull.* **38**, 1783 (2003).
16. L. Zhen, W.S. Wang, C.Y. Xu, W.Z. Shao and L.C. Qin, *Mater. Lett.*, **62**, 1740 (2008).
17. S.L. Gonzalez-Cortes, T.C. Xiao, P.M.F.J. Costa, S.M.A. Rodulfo-Baechler and M.L.H. Green, *J. Mol. Catal. A: Chem.*, **238**, 127 (2005).
18. K.J.D. MacKenzie, J. Temuujin, C. McCammon and M. Senna, *J. Eur. Ceram. Soc.*, **26**, 2581 (2006).
19. A.L.M. de Oliveira, J.M. Ferreira, M.R.S. Silva, S.C. de Souza, F.T.G. Vieira, E. Longo, A.G. Souza and I.M.G. Santos, *J. Therm. Anal. Calorim.*, **97**, 167 (2009).
20. J.T. Kloprogge, M.L. Weier, L.V. Duong and R.L. Frost, *Mater. Chem. Phys.*, **88**, 438 (2004).
21. J.H. Ryu, C.S. Lim, W.C. Oh and K.B. Shim, *J. Ceram. Process. Res.*, **5**, 316 (2004).
22. J. Bi, L. Wu, Z. Li, Z. Ding, X. Wang and X. Fu, *J. Alloys Comp.*, **480**, 684 (2009).
23. S. Das, A.K. Mukhopadhyay, S. Datta and D. Basu, *Bull. Mater. Sci.*, **32**, 1 (2009).
24. K.P.F. Siqueira, R.L. Moreira, M. Valadares and A. Dias, *J. Mater. Sci.*, **4**, 6083 (2010).
25. P. Parhi, T.N. Karthik and V. Manivannan, *J. Alloys Comp.*, **465**, 380 (2008).
26. P. Parhi and V. Manivannan, *J. Eur. Ceram. Soc.*, **28**, 1665 (2008).
27. P. Parhi and V. Manivannan, *J. Alloys Comp.*, **469**, 558 (2009).
28. P. Parhi, S.S. Singh, A.R. Ray and A. Ramanan, *Bull. Mater. Sci.*, **29**, 115 (2006).
29. V. Thangadurai, C. Knittlmayer and W. Weppner, *Mater. Sci. Eng. B*, **106**, 228 (2004).
30. E.G. Gillan and R.B. Kanar, *Chem. Mater.*, **8**, 333 (1996).
31. J.J. Mack, S. Tari and R.B. Kaner, *Inorg. Chem.*, **45**, 4243 (2006).
32. A.M. Nartowski, I.P. Parkin, M. Mackenzie, A.J. Craven and I. MacLeod, *J. Mater. Chem.*, **9**, 1275 (1999).
33. T.K. Mandal and J. Gopalakrishnan, *J. Mater. Chem.*, **14**, 1273 (2004).